Pulsed laser manipulation of an optically trapped bead: Averaging thermal noise and measuring the pulsed force amplitude

Lindballe, Thue Bjerring; Kristensen, Martin V. G.; Keiding, Søren Rud; Stapelfeldt, Henrik; Berg-Sørensen, Kirstine; Keiding, Søren Rud; Stapelfeldt, Henrik

Published in:
Optics Express

Link to article, DOI:
10.1364/OE.21.001986

Publication date:
2013

Document Version
Publisher's PDF, also known as Version of record

Pulsed laser manipulation of an optically trapped bead: Averaging thermal noise and measuring the pulsed force amplitude

Thue B. Lindballe,[1] Martin V. G. Kristensen,[2] Kirstine Berg-Sørensen,[3] Søren R. Keiding,[2,4,5] and Henrik Stapelfeldt[2,5,*]

[1]*Department of Physics and Astronomy, Science and Technology, Aarhus University, DK-8000 Aarhus C, Denmark*
[2]*Interdisciplinary Nanoscience Center, Science and Technology, Aarhus University, DK-8000 Aarhus C, Denmark*
[3]*Department of Physics, FYS-BioComplex, Technical University of Denmark, DK-2800 Kongens Lyngby, Denmark*
[4]*Department of Engineering, Science and Technology, Aarhus University, DK-8200 Aarhus N, Denmark*
[5]*Department of Chemistry, Science and Technology, Aarhus University, DK-8000 Aarhus C, Denmark*
[*]*henriks@chem.au.dk*

Abstract: An experimental strategy for post-eliminating thermal noise on position measurements of optically trapped particles is presented. Using a nanosecond pulsed laser, synchronized to the detection system, to exert a periodic driving force on an optically trapped 10 polystyrene bead, the laser pulse-bead interaction is repeated hundreds of times. Traces with the bead position following the prompt displacement from equilibrium, induced by each laser pulse, are averaged and reveal the underlying deterministic motion of the bead, which is not visible in a single trace due to thermal noise. The motion of the bead is analyzed from the direct time-dependent position measurements and from the power spectrum. The results show that the bead is on average displaced 208 nm from the trap center and exposed to a force amplitude of 71 nanoNewton, more than five orders of magnitude larger than the trapping forces. Our experimental method may have implications for microrheology.

OCIS codes: (070.4790) Spectrum analysis; (110.4280) Noise in imaging systems; (140.3538) Lasers, pulsed; (140.7010) Laser trapping; (170.4520) Optical confinement and manipulation.

References and links

1. R. M. Simmons, J. T. Finer, S. Chu, and J. A. Spudich, "Quantitative measurements of force and displacement using an optical trap," Biophys. J. **70**, 1813–1822 (1996).
2. F. Gittes and C. F. Schmidt, "Signals and noise in micromechanical measurements," Meth. Cell. Biol, **55**, 129–156 (1998).
3. E.-L. Florin, A. Pralle, E. Stelzer, and J. Hörber, "Photonic force microscope calibration by thermal noise analysis," Appl. Phys. A Mater. Sci. **66**, S75–S78 (1998).
4. A. Pralle, E.-L. Florin, E. Stelzer, and J. Hörber, "Local viscosity probed by photonic force microscopy," Appl. Phys. A Mater. Sci. **66**, S71–S73 (1998).

#180399 - $15.00 USD Received 27 Nov 2012; revised 4 Jan 2013; accepted 7 Jan 2013; published 17 Jan 2013

5. K. Berg-Sørensen and H. Flyvbjerg, "Power spectrum analysis for optical tweezers," Rev. Sci. Instrum. **75**, 594–612 (2004).
6. T. Mason, K. Ganesan, J. van Zanten, D. Wirtz, and S. Kuo, "Particle tracking microrheology of complex fluids," Phys. Rev. Lett. **79**, 3282–3285 (1997).
7. F. Gittes, B. Schnurr, P. Olmsted, F. MacKintosh, and C. Schmidt, "Microscopic viscoelasticity: Shear moduli of soft materials determined from thermal fluctuations," Phys. Rev. Lett. **79**, 3286–3289 (1997).
8. T. G. Mason, T. Gisler, K. Kroy, E. Frey, and D. A. Weitz, "Rheology of f-actin solutions determined from thermally driven tracer motion," J. Rheol. **44**, 917–928 (2000).
9. S. Yamada, D. Wirtz, and S. C. Kuo, "Mechanics of living cells measured by laser tracking microrheology," Biophys. J. **78**, 1736–1747 (2000).
10. K. D. Wulff, D. G. Cole, and R. L. Clark, "Servo control of an optical trap," Appl. Opt. **46**, 4923 (2007).
11. A. E. Wallin, H. Ojala, E. Hæggström, and R. Tuma, "Stiffer optical tweezers through real-time feedback control," Appl. Phys. Lett. **92**, 224104 (2008).
12. D. Preece, R. Bowman, A. Linnenberger, G. Gibson, S. Serati, and M. Padgett, "Increasing trap stiffness with position clamping in holographic optical tweezers," Opt. Express **17**, 22718–22725 (2009).
13. S. Tauro, A. Bañas, D. Palima, and J. Glückstad, "Dynamic axial stabilization of counter-propagating beam-traps with feedback control," Opt. Express **18**, 18217–18222 (2010).
14. R. Bowman, A. Jesacher, G. Thalhammer, G. Gibson, M. Ritsch-Marte, and M. Padgett, "Position clamping in a holographic counterpropagating optical trap," Opt. Express **19**, 9908–9914 (2011).
15. Y. Huang, J. Wan, M.-C. Cheng, Z. Zhang, S. M. Jhiang, and C.-H. Menq, "Three-axis rapid steering of optically propelled micro/nanoparticles," Rev. Sci. Instrum. **80**, 063107 (2009).
16. Y. Huang, Z. Zhang, and C.-H. Menq, "Minimum-variance Brownian motion control of an optically trapped probe," Appl. Opt. **48**, 5871–5880 (2009).
17. D. Preece, R. Warren, R. M. L. Evans, G. M. Gibson, M. J. Padgett, J. M. Cooper, and M. Tassieri, "Optical tweezers: wideband microrheology," J. Opt. **13**, 044022 (2011).
18. F. C. Mackintosh and C. F. Schmidt, "Active cellular materials," Curr. Opin. Cell Biol. **22**, 29–35 (2010).
19. T. B. Lindballe, M. V. Kristensen, A. P. Kylling, D. Z. Palima, J. Glückstad, S. R. Keiding, and H. Stapelfeldt, "Three-dimensional imaging and force characterization of multiple trapped particles in low NA counterpropagating optical traps," Journal of J. Eur. Opt. Soc-Rapid **6**, 11057 (2011).
20. H.-U. Ulriksen, J. Thøgersen, S. R. Keiding, I. R. Perch-Nielsen, J. S. Dam, D. Z. Palima, H. Stapelfeldt, and J. Glückstad, "Independent trapping, manipulation and characterization by an all-optical biophotonics workstation," J. Eur. Opt. Soc-Rapid **3**, 08034 (2008).
21. J. C. Crocker and D. G. Grier, "Methods of digital video microscopy for colloidal studies," J. Colloid Interface Sci. **179**, 298–310 (1996).
22. S. C. Chapin, V. Germain, and E. R. Dufresne, "Automated trapping, assembly, and sorting with holographic optical tweezers," Opt. Express **14**, 13095–13100 (2006).
23. S. Keen, A. Yao, J. Leach, R. Di Leonardo, C. Saunter, G. Love, J. Cooper, and M. Padgett, "Multipoint viscosity measurements in microfluidic channels using optical tweezers," Lab Chip **9**, 2059 (2009).
24. P. S. Alves and M. S. Rocha, "Videomicroscopy calibration of optical tweezers by position autocorrelation function analysis," Appl. Phys. B **107**, 375–378 (2012).
25. "The experiment was only carried out at one power of the pulsed laser beam. If the power is reduced (increased) we expect a qualitative similar motion of the bead, following the laser pulse, but with a reduced (increased) maximum displacement from equilibrium due to the weaker (stronger) push from the laser pulse. Beyond a certain power the action on the bead will be so strong that it is pushed out of the optical trap."
26. T. Li, S. Kheifets, D. Medellin, and M. G. Raizen, "Measurement of the Instantaneous Velocity of a Brownian Particle," Science **328**, 1673–1675 (2010).
27. F. Czerwinski, A. C. Richardson, and L. B. Oddershede, "Quantifying noise in optical tweezers by allan variance," Opt. Express **17**, 13255–13269 (2009).
28. S. F. Tolić-Nørrelykke, E. Schäffer, J. Howard, F. S. Pavone, F. Jülicher, and H. Flyvbjerg, "Calibration of optical tweezers with positional detection in the back focal plane," Rev. Sci. Instrum. **77**, 103101 (2006).
29. F. Harris, "On the use of windows for harmonic analysis with the discrete fourier transform," Proc. IEEE **66**, 51–83 (1978).
30. J. Wan, Y. Huang, S. Jhiang, and C.-H. Menq, "Real-time in situ calibration of an optically trapped probing system," Appl. Opt. **48**, 4832–4841 (2009).
31. Y. Huang, P. Cheng, and C.-H. Menq, "Dynamic Force Sensing Using an Optically Trapped Probing System," IEEE ASME Trans. Mechatron. **16**, 1145–1154 (2011).

1. Introduction

In any kind of experiment where an optical trap is used to hold and manipulate a nanometer or micron sized object, the motion of that object will be influenced by stochastic thermal noise.

#180399 - $15.00 USD Received 27 Nov 2012; revised 4 Jan 2013; accepted 7 Jan 2013; published 17 Jan 2013

Much information can be deduced from this thermal noise such as trap characteristics [1–5], viscoelastic properties of polymer solutions [6–8] or of the cellular cytoplasm [9]. At the same time, the thermal noise obscures any deterministic behavior of the trapped object. No matter the precision of the detection system, any tracked motion will appear noisy. Active feedback for force clamping and minimization of the position fluctuations can overcome most of this noise [1,10–14] and, in addition, active feedback methods have been used for trajectory tracking of particles in noisy environments [15,16]. In this paper, we demonstrate a simple experimental strategy utilizing the repeatability of an experimental event to allow for post-elimination of the thermal noise and, through that, identification of an underlying deterministic motion. Post-elimination of the thermal noise is realized by averaging tens or hundreds of single experimental events. This strategy imposes no limitations to the allowed shape of the motion as long as it is deterministic, i. e. the underlying dynamics has to be the same for all experimental events.

The key to repeatability in our experiments is the irradiation of a trapped object by a pulsed laser beam to provide a periodic driving force perpendicular to the trapping laser beam. In practice, this means that the trapped object is pushed away from its equilibrium position in the transversal trapping plane. Thereafter the object returns to its equilibrium position on a time scale determined by the trap characteristics. The period of the push (1 second) is chosen to be significantly longer than the relaxation time to equilibrium (0.4 seconds). The induced motion is similar to that produced using two optical traps in the low frequency viscoelastic studies performed by Preece *et al.* [17]. Although the quantitative evaluation of the viscoelastic moduli in that particular study rely on a questionable estimate of the optical trap strength, it presents an interesting perspective for the current work and demonstrate that precise microrheological measurements can be achieved through optical trapping experiments. Obtaining reliable quantitative microrheological information is a key step in the quest to understand the interplay between active and passive constituents of the cell cytoplasm [18].

In this paper we focus on the post-elimination of thermal noise and characterization of the underlying deterministic motion of a 10 diameter polystyrene bead, held in a counter-propagating optical trap, induced by a 250 nanosecond non-absorbing ($\lambda = 532$ nm) laser pulse. We show that the deterministic motion is measured with a precision of 2 nm corresponding to the noise expected for a bead in a 0.3 K thermal environment. A theoretical description of the deterministic motion is used to determine the trap stiffness. The result agrees very well with a standard autocorrelation analysis of the purely thermal motion of the trapped bead. In addition, we present a model for analysis of the pulsed power spectrum which enables an estimation of the average amplitude of the force exerted by the laser pulses.

2. Experimental setup

In the present setup, the optical trap consists of two counter-propagating infrared laser beams ($\lambda = 1065.5$ nm). The beams originate from a fiber laser (IPG, YLM-20-SC, 20 Watt cw) which is spatially shaped using generalized phase contrast (GPC) optics in combination with a spatial light modulator (SLM), see detailed description in [19]. This produces two individual disc-shaped intensity profiles that are imaged at the focal planes of two objectives (Olympus LMPlan IR 50x, NA 0.55) positioned opposite to each other. The sample cuvette (Hellma Analytics 131-050-40) is placed between these objectives and it contains 10 polystyrene beads suspended in water. The cuvette has a square, 4.2 mm wide profile and the objectives are separated by about 14 mm so that the distance between the two disc-shaped beam profiles is 67 (optical path length). The total power of the two trapping beams is 7.7 mW inside the sample cuvette.

The counter-propagating geometry allows for a large working distance between the two trapping objectives and, consequently, optical access from the side [20]. In these studies we use the sideways access to insert a third objective (Olympus LMPlan IR 20x, NA 0.40), which allows

#180399 - $15.00 USD Received 27 Nov 2012; revised 4 Jan 2013; accepted 7 Jan 2013; published 17 Jan 2013

for the introduction of a 250 nanosecond long, 532 nm laser pulse (Clark-MXR, Inc., ORC-1000), see Fig. 1. In this way, we are able to monitor the behavior of a trapped 10 polystyrene bead as it is exposed to a temporally short but significant force, along the *y*-axis (vertical laboratory axis), i. e. perpendicular to the optical trapping axis (horizontal laboratory axis, the *z*-axis). The energy per pulse at the sample cuvette is 0.038 mJ corresponding to a peak power of 152 W. It is focused to a Gaussian spot size, $\omega_0 = 2$, giving an intensity of 2*e*9.

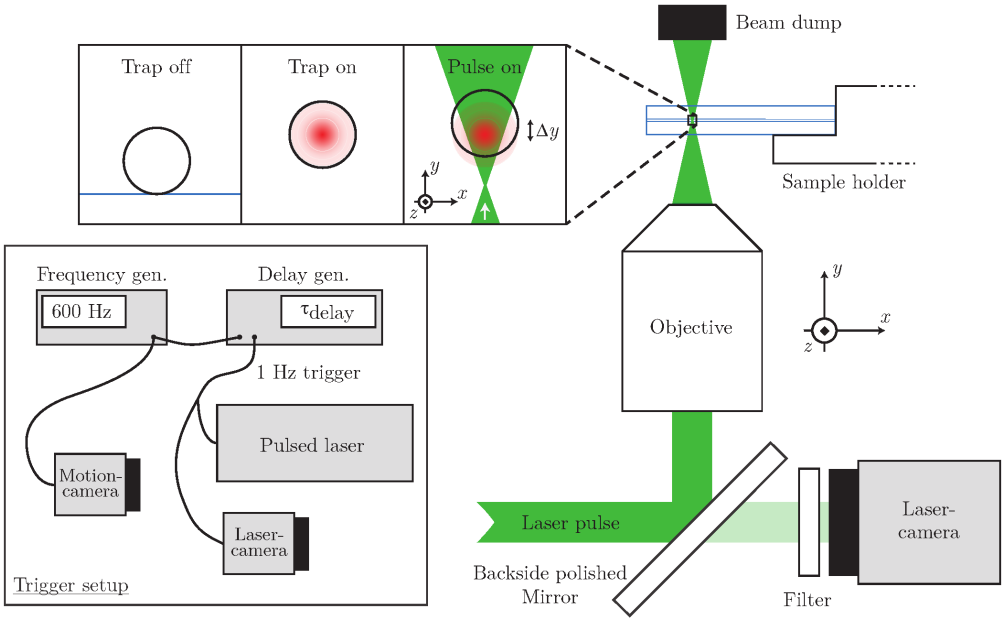

Fig. 1. Schematics showing the pulsed laser setup. The zoom-in on the upper left part shows a cartoon of the experimental procedure described in the main text. This is also the point of view of the motion-camera which monitors the experiment through one of the trapping objectives (not shown). The two counter-propagating trapping beams are aligned along the *z*-axis and are indicated by the red coloring in the cartoon. The inset shows the camera trigger setup.

The bead motion was captured through one of the trapping objectives using a fast camera (Photonfocus MV1-D1312-240-CL-8). An identical camera was used to monitor the intensity variation of the laser pulses. This camera was placed in line with the leak of a backside polished mirror in the pulsed laser path.

A key to the successful elimination of thermal noise is the accurate synchronization between the laser and the motion-camera and, for this reason, the two cameras and the pulsed laser were externally triggered. The motion-camera was operated at a frame rate of $f_{\text{sample}} = 600$ Hz while the laser-camera and the pulsed laser were operated at 1 Hz. The 600 Hz TTL trigger was generated by a frequency generator and used as a common trigger for all three devices, see inset of Fig. 1. To downscale the frequency to 1 Hz we used a delay generator (Stanford Research Systems, Inc., model DG535). Furthermore, the internal delay of the motion-camera was adjusted to temporally locate the pulse-bead interaction prior to the exposure windows of the motion-camera (1.5 ms) and prevent the bead from being in both the equilibrium and a push-displaced position within one frame (the dark time of the camera is 78 microseconds).

The zoom box in Fig. 1 illustrates the procedure of the experiment. First a 10 diameter polystyrene bead was picked up from the bottom of the sample cuvette by the optical trapping

#180399 - $15.00 USD Received 27 Nov 2012; revised 4 Jan 2013; accepted 7 Jan 2013; published 17 Jan 2013

beams and positioned in the center of the cuvette tube, i. e. $\sim$125 away from the cuvette walls. During the first 5 min, the pulsed laser beam is not included and the thermal motion recorded is used to characterize the trap by the correlation method described in Sec. 3 (Eq. (1)). Thereafter, the pulsed laser beam is included for 7.5 min. For each laser pulse the bead is pushed a distance away from equilibrium. The time-dependent bead positions, reflecting the deterministic motion back towards equilibrium, is recorded and, subsequently, analysed and characterized using Eq. (3) and (8) described in Sec. 3.

The bead positions are obtained through post-processing of the captured images. Our tracking algorithm finds the bead by template matching with a Gaussian. It identifies the highest intensity peaks, over a given minimum threshold, as bead centers, and uses a neighborhood-suppression method to ensure that each bead produces only one peak. To obtain sub-pixel accuracy, the positions are refined with a centroid calculation [21, 22]. The computational sub-pixel resolution was estimated by measuring the constant distance between two stuck beads, which produced a Gaussian distribution with a full width at half maximum (FWHM) of $\Delta_{\mathrm{res}} = 7.6 \pm 1.2$ nm.

3. Theory

Assuming a particle is only influenced by the optical trap and the thermal noise, the trap stiffness κ_{corr} along the y-axis can be obtained from its position autocorrelation function, defined as $\langle y(t+\tau)y(t)\rangle$, by fitting this to an exponential function [23, 24],

$$\langle y(t+\tau)y(t)\rangle = Ae^{-\frac{\kappa_{\mathrm{corr}}}{\gamma}\tau}. \tag{1}$$

Here A is the amplitude, γ is the friction coefficient, t is the time, τ is the lag time, and $y(t)$ is the time dependent y-position of the spherically symmetric particle relative to equilibrium, i. e. the center of the trap.

To compare with the standard characterization analysis in Eq. (1) and to evaluate the genuineness of the deterministic dynamics, induced by the laser pulses, we derive an expression for the determination of the trap stiffness from the deterministic particle motion. In general, the particle dynamics is described by the Langevin equation,

$$m\ddot{y} = -\kappa y - \gamma\dot{y} + \xi(t) + \Theta_{t_{\mathrm{p}}}(t), \tag{2}$$

where m is the mass of the trapped particle, κ is the trap stiffness, $\xi(t)$ is the stochastic Brownian force, and $\Theta_{t_{\mathrm{p}}}(t)$ is the pulsed force. The inertial term on the left hand side can be omitted because the characteristic time for loss of kinetic energy through friction, $\tau_{\mathrm{d}} = m/\gamma$, is much shorter than the experimental time resolution, $1/f_{\mathrm{sample}}$. The same relation holds for the duration of the pulsed push and the experimental time resolution. Therefore, we consider the dynamics following the push where the trapped particle is influenced only by the optical trap force and the thermal excitations. Furthermore, the latter is ignored, due to the averaging performed in the post-processing of the tracked positions. When Eq. (2) is solved without the last two terms, the deterministic relaxation of the trapped particle towards its equilibrium position is obtained. The result consists of two exponential terms, and is simplified by the fact that it is fitted to the deterministic behavior of a bead after it is pushed, but before any significant consecutive relaxation in the trap is achieved. For this reason the bead's initial position equals the push length, Δy, and its initial velocity equals zero. In addition to this, the values of the current experimental parameters further simplify the expression, which then reads

$$y(t) = \Delta y \exp\left(-\frac{\kappa_{\mathrm{det}}}{\gamma}t\right), \tag{3}$$

#180399 - $15.00 USD Received 27 Nov 2012; revised 4 Jan 2013; accepted 7 Jan 2013; published 17 Jan 2013

where κ_{det} is the trap stiffness determined from the deterministic bead motion.

An alternative way to investigate the deterministic dynamics is to consider the spectral footprint of the pulsed bead motion. The derivation of an analytical expression for this is based on the full particle dynamics given in Eq. (2). The pulsed force term, $\Theta_{t_{\mathrm{p}}}(t)$, is characterized by the number of pulses, N, the time between them, t_{p}, and the amplitude of the force exerted by the laser pulse on the particle, F_{p}, in the following way:

$$\Theta_{t_{\mathrm{p}}}(t) = F_{\mathrm{p}} \sum_{k=0}^{N-1} h(t - kt_{\mathrm{p}}), \quad h(t) \approx \exp\left(\frac{-t^2}{2\sigma_{\mathrm{p}}^2}\right). \tag{4}$$

Here, it is assumed that the pulse-particle interaction is linearly dependent on the laser intensity and that the temporal shape of the pulses, $h(t)$, is Gaussian with the width σ_{p}. By Fourier transforming each term in Eq. (2) we may obtain an equation for $Y(f)$, which is the Fourier transform of $y(t)$, and from this equation the corresponding power spectrum may be obtained:

$$\left\langle S_y(f) \right\rangle \simeq \frac{Y(f)Y(f)^*}{t_{\mathrm{msr}}}. \tag{5}$$

The Fourier transform of the first four terms are well known and we, therefore, only show the transform of the pulsed force term [Eq. (4)]:

$$\begin{aligned}
\hat{\Theta}_{t_{\mathrm{p}}}(f) &= F_{\mathrm{p}} \int_{-\infty}^{\infty} \sum_{k=0}^{N-1} h(t - kt_{\mathrm{p}}) e^{-i2\pi ft}\, dt \\
&= F_{\mathrm{p}} \left(\sum_{k=0}^{N-1} e^{-i2\pi fkt_{\mathrm{p}}} \right) \int_{-\infty}^{\infty} h(t) e^{-i2\pi ft}\, dt \\
&= F_{\mathrm{p}} \sqrt{2\pi\sigma_{\mathrm{p}}^2}\, e^{-2\pi^2\sigma_{\mathrm{p}}^2 f^2} \sum_{k=0}^{N-1} e^{-i2\pi fkt_{\mathrm{p}}}.
\end{aligned} \tag{6}$$

Within the frequency window determined by the Nyquist frequency the exponential in Eq. (6) will, to a very good approximation, be given by the following expression due to the short duration of the laser pulse ($\sigma_{\mathrm{p}} = 106$ ns):

$$\hat{\Theta}_{t_{\mathrm{p}}}(f) \simeq F_{\mathrm{p}} \sqrt{2\pi\sigma_{\mathrm{p}}^2} \sum_{k=0}^{N-1} e^{-i2\pi fkt_{\mathrm{p}}}. \tag{7}$$

With these assumptions, we can derive the pulsed power spectrum from Eq. (2),

$$\left\langle S_y(f) \right\rangle \simeq \frac{1}{2\pi^2} \frac{D + \frac{\pi\sigma_{\mathrm{p}}^2 F_{\mathrm{p}}^2}{\gamma^2 t_{\mathrm{msr}}} \frac{\sin^2(\pi N t_{\mathrm{p}} f)}{\sin^2(\pi t_{\mathrm{p}} f)}}{f_{\mathrm{c}}^2 + f^2}. \tag{8}$$

Here, D is the diffusion constant, t_{msr} is the total duration of the measurement, and f_{c} is the corner frequency, which is related to the trap stiffness through the relation $\kappa = 2\pi\gamma f_{\mathrm{c}}$.

As will be shown in Sec. 5, it is possible to get a very precise measurement of the repetition frequency of the laser pulses, $f_{\mathrm{p}} = 1/t_{\mathrm{p}}$. In addition, F_{p} can be estimated through Eq. (8). This is possible since the other variables are easily measured or estimated by other methods. Furthermore, F_{p} may be used to get an estimate of Δy, for comparison with the one found through Eq. (3). This is achieved by noticing the temporal separation of the relevant time scales. The characteristic relaxation time of the trap is $\tau_{\mathrm{t}} = \gamma/\kappa \sim 0.09$ s; the momentum relaxation time of the water-suspended bead is $\tau_{\mathrm{d}} \sim 6$; and the acceleration time of the particle, i. e. the

#180399 - $15.00 USD Received 27 Nov 2012; revised 4 Jan 2013; accepted 7 Jan 2013; published 17 Jan 2013

duration of the laser pulse, is $2\sigma_p \sim 0.2$. As such, the induced peak velocity due to the laser pulse is given by the integral of a Gaussian with a width of σ_p, and an amplitude of F_p/m. Then Δy is obtained from the integral of the velocity which starts at the induced peak value and decays exponentially with characteristic time τ_d:

$$\Delta y^2 \approx \frac{2\pi\sigma_p^2 F_p^2}{\gamma^2}. \tag{9}$$

Note that Δy and F_p are determined by Eq. (3) and Eq. (8) respectively and only in the case where τ_t, τ_d, and $2\sigma_p$ are temporally separated can they be related through Eq. (9). The temporal and spectral analyses, expressed by Eq. (3) and (8) respectively, are, thus, supplementary and provide two different pieces of insight regarding the deterministic dynamics.

4. Post-eliminating thermal noise

Figure 2 shows the y-position of the bead with and without the pulsed laser. The dominance of the thermal noise obscures any clear indication of the repetitive motion induced by the laser pulses. The laser pulses are, however, precisely timed with respect to the recording of the bead position so the data can be divided into 450 equally sized pieces containing one pulse-bead-interaction event each. Averaging the 450 events gives an effective post-elimination of the thermal noise - see Fig. 3. The averaged bead motion appears highly deterministic [25] which is supported by the very good agreement with a fit of Eq. (3). From the fit the trap stiffness, $\kappa_{\mathrm{det}_{450}} = 1.16 \pm 0.01$ and the push length, $\Delta y_{450} = 207 \pm 1$, were obtained. Also, we estimated the peak velocity, v_0, of the bead, resulting from the action of the laser pulse, by assuming that no significant decay of the velocity takes place before the laser pulse is over. Then v_0 can be determined by solving the integral $\Delta y = \int_0^\infty v_0 \exp(-t/\tau_d)\, dt$ which gives $v_0 = \Delta y/\tau_d$. The result, $v_0 = 34$ mm/s, is about 400 times the average velocity due to the Brownian motion (0.086 mm/s). Direct information about the instantaneous velocity of the bead may be possible by implementing a recently reported method on velocity measurements of particles trapped with counter-propagating laser beams [26].

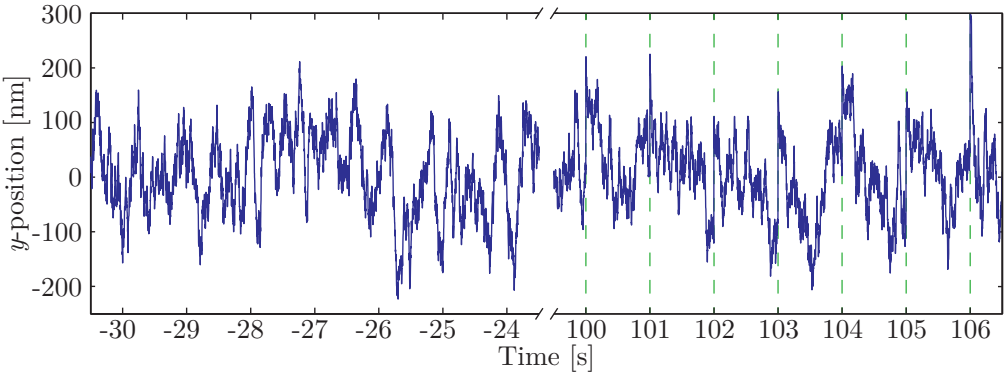

Fig. 2. Bead position as a function of time with and without the pulsed laser included. The vertical dashed lines indicate the positions of the pulse-bead interaction events. The first pulse is located at time $t = 0$ s.

To asses the experimental uncertainty on the deterministic measurement the averaging was performed on 45 events, see example in the insets of Fig. 3. This provides ten independent measurements of the deterministic motion and the standard deviations of κ_{det} and Δy could be calculated. From the fit of Eq. (3), $\kappa_{\mathrm{det}_{45}} = 1.19 \pm 0.24$ and $\Delta y_{45} = 208 \pm 19$ were obtained.

#180399 - $15.00 USD Received 27 Nov 2012; revised 4 Jan 2013; accepted 7 Jan 2013; published 17 Jan 2013

From the images recorded with the laser camera the standard deviation of the pulse intensity was determined to be < 2 % and hence could be neglected.

For comparison with the deterministic result, the trap stiffness was determined with Eq. (1). From a calculation of the Allan variance on the purely thermal data, i. e. the 5 min long section recorded prior to the inclusion of the pulses, an optimal data length of 17 seconds was determined [27]. This provides 17 independent position measurements and by fitting the corresponding autocorrelation functions, like the one in Fig. 4, with Eq. (1) (red line) the trap stiffness, $\kappa_{\text{corr}} = 1.12 \pm 0.11$ was obtained.

The agreement of the deterministic model in Eq. (3) and the averaged data together with the agreement of the trap stiffness values, κ_{det} and κ_{corr}, corroborates our interpretation of the trace in Fig. 3 as representing the real deterministic bead motion. To determine the extent with which the thermal noise has been eliminated, the variation of the y-position relative to the model, i. e. the y-position subtracted the fit, was considered. The standard deviation of the relative y-position for the 450-event average is $\sigma_{\text{avg}_{450}} = 2.0$ nm. Together with the trap stiffness this value can be used to calculate a corresponding (virtual) thermal noise temperature of the system. The result, $T_{\text{N}_{450}} = \kappa\sigma^2_{\text{avg}_{450}}/k_{\text{B}} = 0.3$ K, states that without averaging, a temperature this low is required to be able to measure the trace in Fig. 3 (obviously not an experimentally possible scenario for the water-suspended bead). The experimental strategy, thus, reduced the stochastic-motion-temperature of the trapped bead from room temperature to a sub-Kelvin temperature.

The elimination of thermal noise can also be evaluated by comparing the thermal motion of the bead and the precision with which the deterministic motion has been measured. The size of the measured thermal bead motion was determined both from the purely thermal data and the pulsed data, see error bars in inset of Fig. 3, and was found to be $\sigma_{\text{therm}} = 68.6 \pm 2.2$ nm. This is more than 30 times higher than the value of $\sigma_{\text{avg}_{450}}$, which states that a deterministic bead motion of a few nanometers can be identified and separated from a thermal motion of several tens of nanometers.

The precision of the 45-event average is $\sigma_{\text{avg}_{45}} = 8.0 \pm 1.6$ nm which correspond to a noise temperature of $T_{\text{noise}_{45}} = 5.2 \pm 2.1$ K. It is clear that an increase in the number of averaged

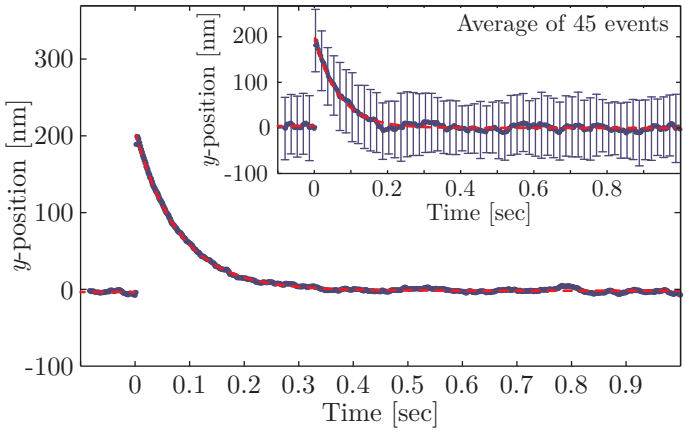

Fig. 3. Plot of the bead's averaged y-position as a function of time (blue dots). Averaging 450 events like the seven shown in Fig. 2 gave this result. The inset shows the same for the average of 45 events including error bars (shown for every tenth data point), which indicate the standard deviation of the 45 measurements, i. e. the magnitude of the thermal motion. The fits of Eq. (3) are shown by the red dashed lines. They are almost indistinguishable from the data.

#180399 - $15.00 USD Received 27 Nov 2012; revised 4 Jan 2013; accepted 7 Jan 2013; published 17 Jan 2013

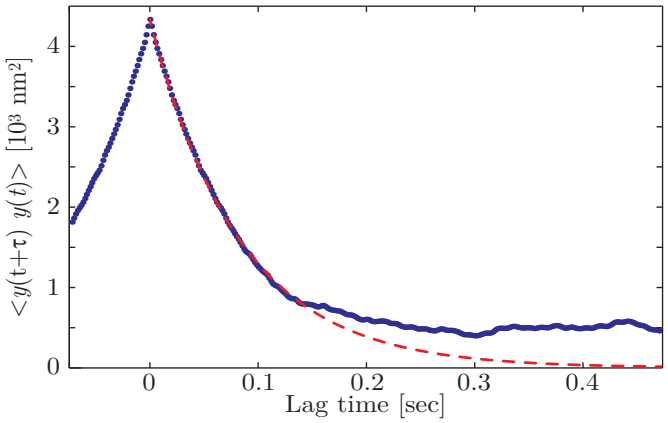

Fig. 4. Example of the position correlation function (dots) of a 17 second long data section without the laser pulses. The fit of Eq. (1) (red dashed line) was performed for $0 < \tau < 1.2\tau_t = 0.1$ s.

events can significantly enhance the position precision and the elimination of the thermal noise. At the same time, a relatively small number of events is required to make the deterministic motion appear, see inset of Fig. 3, depending on the amplitude of the deterministic motion of course.

5. The pulsed power spectrum

From a spectral analysis of the pulsed bead motion additional information about the underlying dynamics can be obtained. The amplitude of the force exerted by the laser pulses on the bead was determined by fitting the pulsed power spectrum model, Eq. (8), to the measured spectrum. Figure 5 shows excellent agreement between the measurement (blue line) and the fit (red dashed line) in the range $0 < f < 50.5$. The fit directly yields the amplitude of the force, $F_p = 70.9$, which is more than five orders of magnitude larger than the trapping force, $F_t < \kappa\Delta y \approx 0.3$. A combination of a short duration of the push and the energy dissipation, i. e. the viscosity and drag coefficient, retain the bead within the trap. While a laser pulse is present, the trapping force is completely negligible.

Determining the force from the fit could give rise to great uncertainty due to the scarce number of data points forming the peaks, see Fig. 5(b)–5(c). To investigate this, the force amplitude was calculated for individually measured values of the peak power. In accordance with Tolić-Nørrelykke *et al.* the measuring time, t_{msr}, was chosen to be an integer multiple of the pulse period, t_p, to obtain a measured spectrum where the peaks are described by a single data point [28, 29]. This justifies the calculation of the pulsed force amplitude from each individual peak in the measured spectrum using the theoretical expression for the (absolute) peak power. At the peak positions, $f_{peak,i}$ with $1 \leq i \leq 50$, the spectrum in Eq. (8) reduces to

$$\left\langle S_y(f_{peak,i})\right\rangle \approx \frac{1}{2\pi^2}\frac{D+\frac{\pi N\sigma_p^2 F_p^2}{\gamma^2 t_p}}{f_c^2+f_{peak,i}^2} \tag{10}$$

where only F_p is unknown. The pulse width, σ_p, was measured with a photodiode and everything else was determined by fitting the non-pulsed power spectrum model, Eq. (8) without the pulsed term, to the measured spectrum with the peaks (and five point on each side) manually excluded. Equation (10), thus, enable the calculation of the force directly from each measured

#180399 - $15.00 USD Received 27 Nov 2012; revised 4 Jan 2013; accepted 7 Jan 2013; published 17 Jan 2013

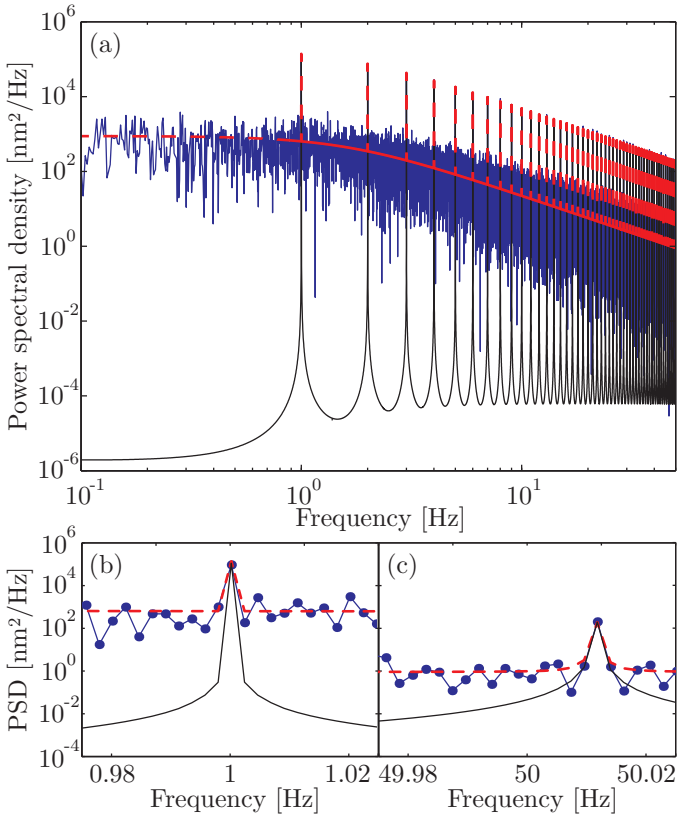

Fig. 5. (a) The measured power spectrum of the bead motion when subject to the laser pulses (blue line). The red dashed line is a fit of Eq. (8). The black line is a plot of the periodic pulsed part of the fit. (b)–(c) Closeup of the peaks at 1 Hz and 50 Hz respectively (connected blue dots). The pulse rate was found to be $f_p = 1.0002$ Hz.

power spectrum peak. The result, $F_p = 70.9 \pm 4.3$, consolidates the force amplitude determined from the fit of the pulsed power spectrum model in Eq. (8).

The result of the spectral and the temporal analyses is compared through Eq. (9). The estimate of the push length from the force, $\Delta y_{F_p} = 209 \pm 13$, shows very good agreement between the two analyses. Consequently, the temporal separation of the relevant characteristic times, τ_t, τ_d, and $2\sigma_p$, was satisfied in this experiment, as argued in Sec. 3.

Equation (9) can also be used to estimate the smallest push length needed to obtain visible peaks in the spectrum so that a force fit is viable. Setting the two terms on the right hand side of Eq. (10) equal, we obtain the relation

$$\Delta y_{\min} = \sqrt{\frac{2Dt_p}{N}}, \tag{11}$$

where $t_{msr} = Nt_p$ have been inserted. In words, the minimum push length needed to enable the determination of the push force amplitude is proportional to the free diffusion of the particle between two subsequent laser pulses. The proportionality factor, $1/\sqrt{N}$, states that an increase in the number of pulses increase the sensitivity of the fit. For the present experimental parameters $\Delta y_{\min} = 14$ nm.

#180399 - $15.00 USD Received 27 Nov 2012; revised 4 Jan 2013; accepted 7 Jan 2013; published 17 Jan 2013

6. Concluding remarks

Post-elimination of the thermal noise on the motion of an optically trapped 10 polystyrene bead proved successful. The thermal motion was reduced from ∼68 nm to ∼2 nm, corresponding to the thermal noise at room temperature and at 0.3 K respectively. This enabled imaging of the deterministic motion as it decays, within 0.4 seconds, from an initial distance of ∼208 nm away from equilibrium to the equilibrium position in the trap. A comparison of the deterministic model and the data corroborated the assignment of the averaged bead motion as being the true deterministic motion. This was further supported by a comparison of the trap stiffness values determined from this motion and from the autocorrelation function of the purely thermal part of the data, respectively.

The elimination of the thermal noise was achieved by using a pulsed laser beam to impose a periodic motion of the trapped bead. Because the laser pulses were precisely timed with respect to the recording of the bead position, the data could be divided into sections containing one laser induced motion each. The thermal noise could subsequently be strongly reduced by averaging all recorded position traces of the identical events. The spatial resolution can, in principle, be made arbitrarily high by increasing the number of events. When the motion studied cannot be repeated and, therefore, the post-averaging method cannot be applied, methods based on real-time processing will provide useful alternatives for extracting particle trajectories from the thermal noise [30, 31].

A theoretical expression for the power spectrum of the pulsed bead motion including the thermal noise was presented. A fit of this expression enabled the determination of the push force amplitude. With a value of ~ 71 nanoNewton it is five orders of magnitude larger than the optical trapping forces.

Using an independent laser to push a trapped object, has several advantages over other possible driving force methods, such as using a piezo-stage or an additional optical trap [17]. Here we used a sideways geometry, enabled by a counter-propagating beams trap, for the push laser beam but it may also be possible to bring in the push laser beam coaxial with the trapping laser beam in a single beam trap and study the laser induced particle displacement along the trapping axis. In principle, the laser pulses have no limits on the duration, ranging from femtoseconds to hundreds of nanoseconds or longer. Furthermore, the laser wavelength and polarization can be changed, bringing several adjustable parameters to the setup. Parameters like these have interesting perspectives for combining the current experimental setup with studies of photochemistry and cells. For example, the dependence of the push force and the subsequent dynamics on the laser parameters can be studied.

Also, our experimental strategy may be used to extend a recently reported wideband analysis of viscoelastic media [17] to include spectral information in the range.

Acknowledgments

This work is supported by the Danish Technical Scientific Research Council (FTP) and the Siemens Foundation. We would like to acknowledge Bent Ørsted for a number of helpful discussions on the derivation of the pulsed power spectrum model.

#180399 - $15.00 USD Received 27 Nov 2012; revised 4 Jan 2013; accepted 7 Jan 2013; published 17 Jan 2013